Photoelectron spectroscopy of NpPd$_3$ and PuPd$_3$

M D Le[1], H C Walker[1], K A McEwen[1], T Gouder[2], F Huber[2] and F Wastin[2]

[1] Department of Physics and Astronomy, and London Centre for Nanotechnology, University College London, Gower Street, London, WC1E 6BT, UK
[2] European Commission, Joint Research Centre, Institute for Transuranium Elements, Post Box 2340, D-76125 Karlsruhe, Germany

Abstract.
We present the results of x-ray and ultra-violet photoelectron spectroscopy of NpPd$_3$ and PuPd$_3$. The spectra indicate that for both compounds, the $5f$ electrons are well localised on the actinide sites. Comparison with bulk measurements indicates that for NpPd$_3$ the electrons have a valence of Np^{3+} and thus a ground state $5f^4$ with a Hund's rules $^5I_4$ configuration. Similarly for PuPd$_3$, we find a Pu^{3+} valence, $5f^5$ ground state and a Hund's rules $^6H_{5/2}$ configuration.

PACS numbers: 79.60.-i, 75.50.Ee
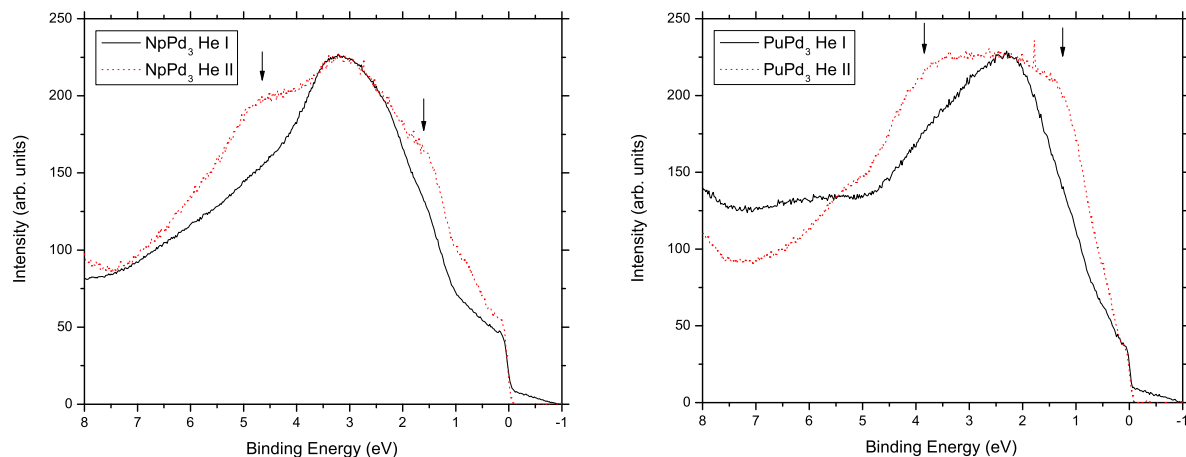
1. Introduction

NpPd$_3$ crystallises in the cubic AuCu$_3$ and double-hexagonal close-packed (dhcp) structures, whereas PuPd$_3$ crystallises only in the cubic AuCu$_3$ structure. Both compounds have been studied using bulk measurements and neutron diffraction [1, 2]. These measurements show that the cubic compounds are antiferromagnetic, NpPd$_3$ below $T_N = 55$ K with an ordered moment of 2.0 μ_B per Np atom, whilst PuPd$_3$ orders below $T_N = 24$ K with a moment of 0.8 μ_B per Pu atom. The lattice parameter and actinide-actinide distances in both cubic (4.095Å) and dhcp (4.072 Å) NpPd$_3$ and PuPd$_3$ (4.105Å) are similar, and above the critical distance at which the $5f$ moments are expected to be localised [3].

The measured paramagnetic effective moments of 2.74 μ_B/Np-atom for cubic NpPd$_3$ and 2.83 μ_B/Np-atom for dhcp NpPd$_3$ suggests that the ground state is $5f^4$, whereas for PuPd$_3$, the measured paramagnetic effective moment of 1.06 μ_B per Pu-atom suggests that the ground state is probably $5f^5$. We have performed photoelectron spectroscopy on thin film samples, prepared in-situ by sputter deposition from NpPd$_3$ and PuPd$_3$ targets made by arc-melting at the ITU. The target samples had been used to measure the bulk properties of these systems and synthesis details may be found in references [2, 4].

2. Experimental Details and Results

The photoelectron spectroscopy was performed in a spectrometer equipped with a Leybold LHS 10 hemispherical analyser, placed in a dedicated transuranium glovebox. The analysis chamber (base pressure 4×10^{-10} mbar) is connected to the preparation chamber (base pressure 3×10^{-9} mbar) within the glovebox and samples were analysed as soon as the deposition was complete. Figure 1 shows the ultraviolet photoelectron spectra (UPS) obtained from He I and He II excitation radiation ($h\nu = 21.22$ and 40.81 eV respectively) produced by a windowless UV rare-gas discharge source. The energy resolution is approximately 45meV. He II radiation is more sensitive to the $5f$ photoexcitation, whereas this cross-section is relatively weak for He I radiation. Thus the extra bulge in the PuPd$_3$ He II spectra at around 1 eV binding energy with respect to the He I spectra shows that this emission is of $5f$ origin. If the $5f$ electrons in NpPd$_3$ and PuPd$_3$ were itinerant, we should expect to observe significant spectral weight in the He II spectra at the Fermi energy. This is not observed in the data. Instead the $5f$ emissions are shifted to approximately 1.5 eV binding energy in NpPd$_3$ and 1 eV in PuPd$_3$, indicating that they are well localised. This is in agreement with previous studies of $5f$ localisation in Pu metal [5].

The shoulders at 5 eV in the NpPd$_3$ valence band spectra and at 4 eV in the PuPd$_3$ spectra are attributed to the $2p$ emissions from surface oxygen impurities, due for example to the adsorption of water or CO, because their intensity grows with time and with non-optimal deposition conditions. The emission is larger in He II than in He I, despite the lower O-$2p$ cross-section for He II radiation [6]. This may be explained by the enhanced surface sensitivity of He II radiation which has an attenuation length of 1 monolayer versus 3-5 monolayers for He I radiation and thus probes preferentially adsorbed species. There is no evidence of any oxide formation on the surface since we did not detect any higher binding energy satellites in the core level $4f$ spectra of NpPd$_3$ or PuPd$_3$ similar to those observed in
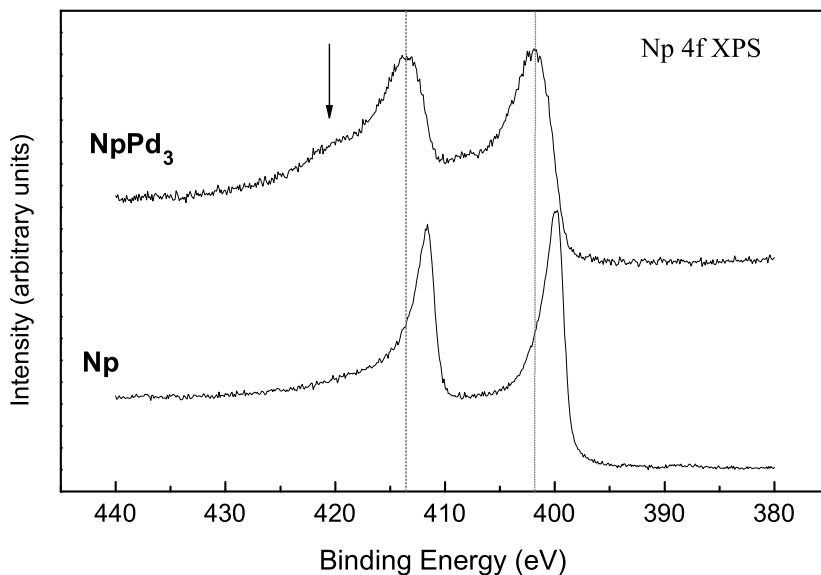

Figure 1. Valence band structure of NpPd$_3$ and PuPd$_3$ for photon energy $h\nu = 21.22$ eV (He I, solid black line) and $h\nu = 40.81$ eV (He II, dotted red line). The arrows indicates features in the He II spectra discussed in the text.

the actinide dioxides [7]. The broad maximum around 3 eV binding energy, present in both He I and He II spectra, is due to the Pd-$3d$ excitations.

Figures 2 and 3 show the x-ray photoelectron spectra (XPS), taken using Al-K$_\alpha$ radiation with the same spectrometer described above. The energy resolution is $\approx$1.0 eV. Figure 2 shows the neptunium $4f$ core level transitions, whilst figure 3 shows the plutonium $4f$ transitions.

For comparison, the figures also show reference spectra for Np and α-Pu which are the delocalised cases. The spectra of both compounds are shifted to about 3 eV higher binding energy, compared to the metallic cases. A similar behavior was observed for UPd$_3$ and U, which was taken as evidence for $5f$ localisation and explained by the screening model [8]. In this model, the $5f$ states, upon localisation, lose their capability to screen the photohole which is created after emission of the $4f$ electron. Screening is instead performed by the extended ds-states. However, this screening is less efficient, due to the larger size of the ds orbitals, and results in a displacement of the photoemission line to higher binding energy (BE). Close to the localisation threshold (for weakly hybridised f-states) both screening types may co-exist, as e.g. in α-Pu, where the ds-screened peak appears as a high BE satellite on the f-screened (well screened) main line (Fig. 3). In Np metal (Fig. 2), no high BE satellite is observed showing the $5f$ states to be well delocalised. But in both compounds, all intensity is shifted to the high BE position, which shows the $5f$ states to be well localised. It is to be noted that the peaks in the $4f$ core spectra of PuPd$_3$ actually coincide quite closely with the poorly screened
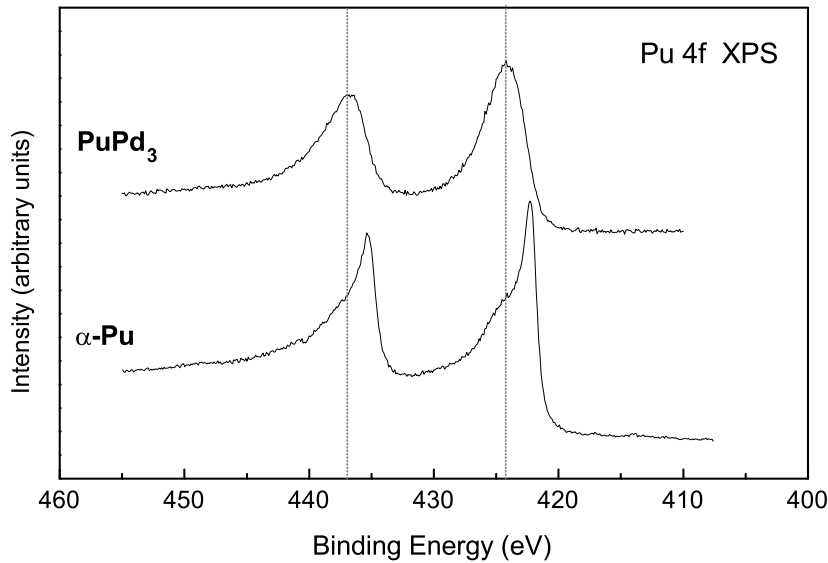

Figure 2. Np-$4f$ spectra for NpPd$_3$. The two peaks represent transitions from the $4f_{5/2}$ and $4f_{7/2}$ core levels at binding energies 413.8eV and 402.3eV respectively. The dotted line is a guide to the eye. The arrow indicates a feature discussed in the text.
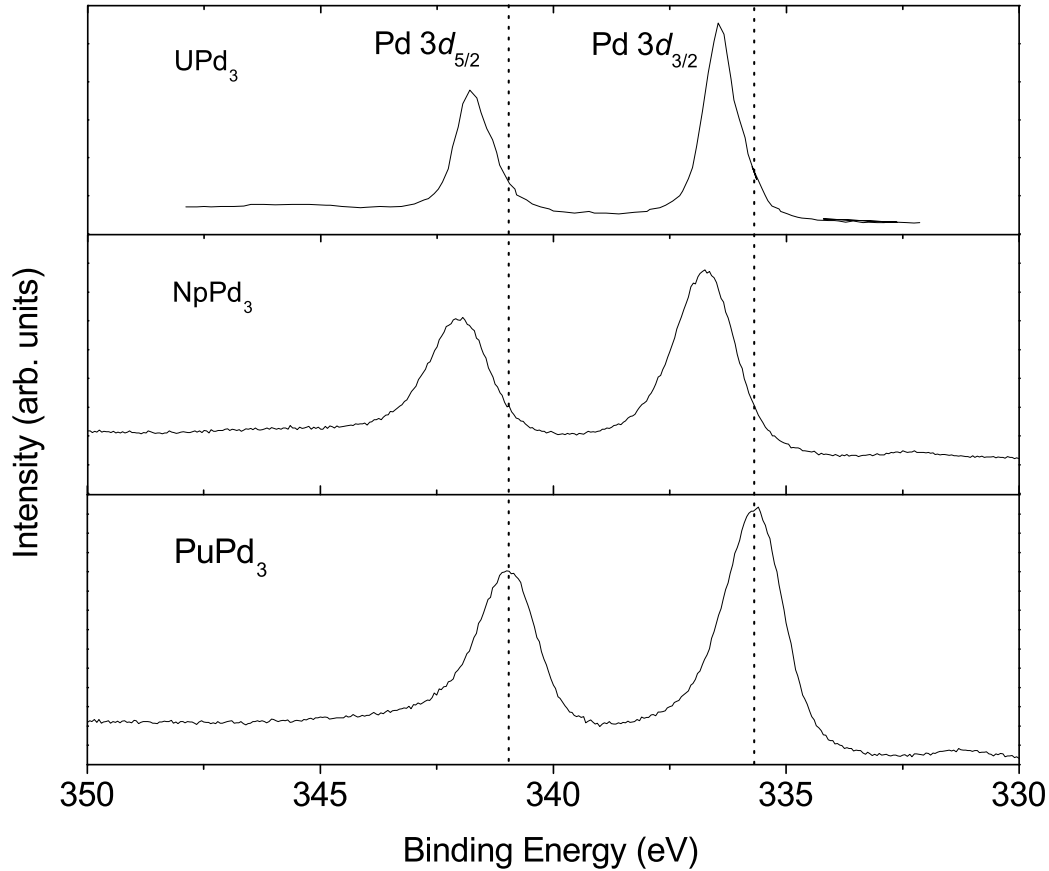
3

peaks in α-Pu.

Supplementary indication for $5f$ localisation is provided by the broadened shape of the $4f$ emission in the compounds, compared to the pure metals, which is due to exchange splitting between the $4f$ hole and the localised $5f$ states that is not resolved. This is analogous to the splitting of the s core levels of the rare earths by the $4f$ states [9]. Similar broadening is observed between U and Am, and explained by the $5f$ localisation in Am metal [10]. In addition, the $4f$ peaks in both Np and α-Pu show an asymmetric shape which is due to $e - h$ pair formation of conduction electrons from scattering by the core-hole potential [11]. This is directly proportional to the density of states at the Fermi level. Thus the symmetrical shape of the $4f$ emission in the compounds compared to the metal shows that the DOS at E_F is drastically reduced. This directly correlates with $5f$ localisation and is consistent with the valence band spectra in Fig. 1, where the $5f$ states are shown to be shifted away from the Fermi-level.

The $4f$ XPS spectra in NpPd$_3$ also exhibits a satellite at about 7 eV higher binding energy than the main $4f_{5/2}$ peak as indicated by the arrow in Figure 2. Similar satellites for both the $4f_{5/2}$ and $4f_{7/2}$ spin orbit components were also observed in many localised uranium compounds [12], including UPd$_3$ [13], and also in NpO$_2$ [14]. Using the Anderson impurity model, the satellites may be attributed to a final state which is an antibonding mixture of the $4f^{13}5f^n$ and $4f^{13}5f^{n+1}$ configurations ($n = 4$ for Np), mixed by fd hybridisation, whereas the main line is due to a bonding mixture. That satellites are not observed in the $4f$ spectra

Figure 3. Pu-$4f$ spectra for PuPd$_3$. The two peaks represent transitions from the $4f_{5/2}$ and $4f_{7/2}$ core levels at binding energies 437.7eV and 424.9eV respectively. The dotted line is a guide to the eye.

4

Figure 4. X-ray photoelectron spectra of the core Pd $3d$ levels in UPd$_3$, NpPd$_3$, and PuPd$_3$. Note that UPd$_3$ crystallises in the hexagonal TiNi$_3$ structure, whereas the spectra shown for NpPd$_3$ and PuPd$_3$ are from samples with the cubic AuCu$_3$ structure.

in PuPd$_3$ may indicate that the $4f^{13}5f^n$ ($n = 5, 6$) configurations in PuPd$_3$ have larger energy separations and so are more weakly mixed.

Finally, figure 4 shows the Pd $3d$ core levels for UPd$_3$, NpPd$_3$ and PuPd$_3$, and the chemical shift in energies between the different compounds. There is a shift of ≈ 1 eV between the levels of NpPd$_3$ and PuPd$_3$, and a shift of ≈ 0.3 eV between NpPd$_3$ and UPd$_3$. These small shifts in the binding energy may indicate slight changes of screening of the core Pd electrons in the different compounds.

In conclusion, we have measured the photoelectron spectra of NpPd$_3$ and PuPd$_3$, showing that the valence and core-level spectra are both consistent with a picture of localised $5f$ electrons, in agreement with measurements of the bulk properties of these compounds.

5

Acknowledgments

References

[1] Nellis W J, Harvey A R, Lander G H, Dunlap B D, Brodsky M B, Mueller M H, Reddy J F and Davidson G R 1974 *Phys. Rev. B* **9** 1041

[2] Walker H C, McEwen K A, Boulet P, Colineau E, Griveau J-C, Rebizant J and Wastin F 2007 *Phys. Rev. B* **76** 174437

[3] Hill H H 1970 *Nucl. Metall.* **17** 2

[4] Le M D, McEwen K A, Wastin F, Boulet P, Colineau E, Jardin R, and Rebizant J 2008 *Physica B* **403** 1035

[5] Havela L, Gouder T, Wastin F and Rebizant J 2002 *Phys. Rev. B* **68** 235118

[6] Yeh J J and Lindau I 1985 *Atomic Data and Nuclear Data Tables* **32** 1

[7] Veal B W, Lam D J, Diamond H, and Hoekstra H R 1977 *Phys. Rev. B* **15** 2929

[8] Fuggle J C, Campagna M, Zolnierek Z and Lässer R 1980 *Phys. Rev. Lett.* **45** 1597

[9] Cohen R L, Wertheim G K, Rosencwaig A, Guggenheim H J 1972 *Phys. Rev. B* **5** 1037

[10] Naegele J R, Manes L, Spirlet J C, Müller W 1984 *Phys. Rev. Lett.* **52** 1834

[11] Mahan G D 1967 *Phys. Rev.* **163** 612

[12] Allen J W, Kand J S, Lassailly Y, Maple M B, Torikachvili M S, Ellis W, Pate B and Lindau I 1987 *Solid State Commun.* **61** 183

[13] Imer J M, Malterre D, Grioni M, Weibel P, Dardel B and Baer Y 1991 *Phys. Rev. B* **44** 10455

[14] Gunnarsson O, Sarma D D, Hillebrecht F U and Schönhammer K 1988 *J. Appl. Phys.* **63** 3676